Effect of pH on in-electrospray hydrogen/deuterium exchange of carbohydrates and peptides

Jacob B. Hatvany, O. Tara Liyanage [#] , Elyssia S. Gallagher*
Department of Chemistry & Biochemistry, Baylor University, One Bear Place #97348, Waco
TX 76798
*Corresponding author:
Elyssia S. Gallagher
Elyssia_gallagher@baylor.edu
#Current address:
O. Tara Liyanage
Amgen Inc., 360 Binney St., Cambridge, MA, 02141

Abstract: Carbohydrates are critical for cellular functions as well as an important class of metabolites. Characterizing carbohydrate structures is a difficult analytical challenge due to the presence of isomers. In-electrospray – hydrogen/deuterium exchange – mass spectrometry (in-ESI HDX-MS) is a method of HDX that samples the solvated structure of carbohydrates during the ESI process and requires little to no instrument modification. Traditionally, solution-phase HDX is utilized with proteins to sample conformational differences, and pH is a critical parameter to monitor and control due to the presence of both acid- and base-catalyzed mechanisms of exchange. For In-ESI HDX, the pH surrounding the analyte changes before and during labeling, which has the potential to affect the rate of labeling for analytes. Herein, we alter the pH of spray solutions containing model carbohydrates and peptides, perform in-ESI HDX-MS, and characterize the deuterium-uptake trends. Varying pH results in altered D uptake, though the overall trends differ from the expected bulk-solution trends due to the electrospray process. These findings show the utility of varying pH prior to in-ESI HDX-MS for establishing different extents of HDX as well as distinguishing labile functional groups that are present in different analytes.

1. Introduction

Carbohydrates, also referred to as glycans, play crucial roles in biology, including in cellular communication¹⁻³ and immune responses.⁴ This class of molecules forms common metabolites and also serves as biomarkers for disease states.^{5,6} Due to their biological relevance, there is a need to analyze the structures of these molecules, often in complex mixtures of other metabolites, including peptides and small molecules.^{7,8} Yet, carbohydrates are challenging to analyze due to isomerism, including variations in monosaccharide structures (epimers), locations of glycosidic bonds (regioisomers), configurations of glycosidic bonds (stereoisomers), and the non-linear nature of polysaccharide composition (branching).

Hydrogen/deuterium exchange (HDX) coupled to mass spectrometry (MS) is a technique that has been used both to distinguish small molecule isomers as well as to analyze the conformations and dynamics of biomolecules. HDX-MS has primarily been used to analyze proteins, ^{9, 10} but has also been applied to other molecules, including peptides, ¹¹ oligonucleotides, ¹² metabolites, ^{8, 13} and carbohydrates. ^{12, 14-24} Towards the analysis of carbohydrates, HDX labeling has been performed in the solution-phase, ¹⁵ gas-phase, ^{18, 25, 26} and during ionization, prior to MS detection, using electrospray ionization (ESI), ^{16, 17, 19-23} matrix-assisted LASER desorption/ionization (MALDI), ¹⁴ capillary vibrating sharp-edge spray ionization (cVSSI), ²⁷ and conductive polymer spray ionization (CPSI). ²⁸

In-ESI HDX-MS is uniquely suited for analyzing carbohydrates.²¹ During ESI, a Taylor cone forms due to application of a potential, resulting in the generation of ESI droplets containing carbohydrates and solvent (**Figure 1**). These carbohydrate-containing ESI droplets are exposed to deuterating reagents, in this case, D₂O vapor, within the ESI source. We

hypothesize that D₂O condenses into the ESI droplets,^{21, 24} enabling HDX labeling of solvated carbohydrates. Upon complete desolvation of the ESI droplets, neutral carbohydrates adduct to metal ions, improving the ion signal for MS detection.²⁹ Additionally, gas-phase HDX of carbohydrate-metal adducts is significantly reduced, essentially quenching the HDX labeling reaction when gas-phase, metal-ion adducts form.^{21, 30} Desolvation during ESI occurs on a timescale of microseconds to milliseconds.³¹ HDX labeling of hydroxyls, the primary, labile functional group within carbohydrates, undergoes exchange on a similar, rapid timescale.^{32, 33} Thus, labeling carbohydrates during ESI enables the analysis of solvated carbohydrates, sampling biologically relevant conformations.

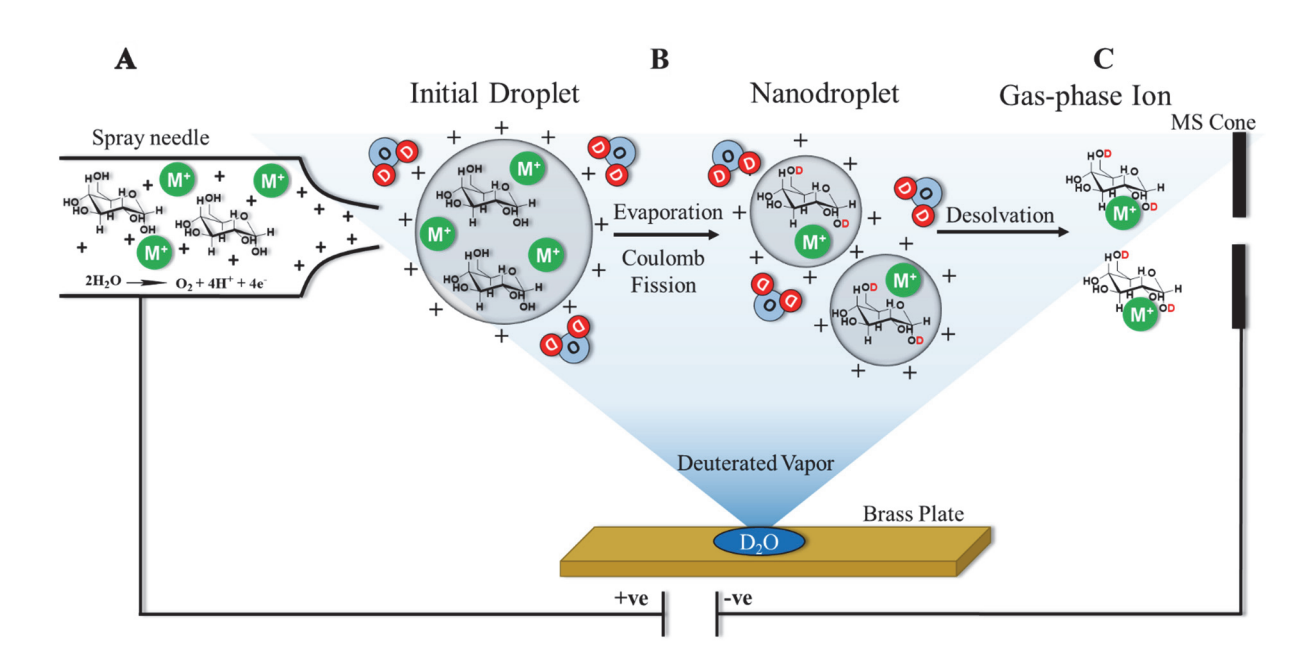


Figure 1. Diagram of in-ESI HDX showing (A) electrochemical reactions that influence pH within the spray needle, (B) pH increasing during droplet desolvation as H⁺ ions are concentrated in evaporating droplets while HDX reactions occur within ESI droplets, and (C) analyte ionization to form carbohydrate-metal adducts. Adapted from Gass, DT, Quintero, AV, Hatvany,

JB, Gallagher, ES. Metal adduction in mass spectrometric analyses of carbohydrates and glycoconjugates. *Mass Spectrometry Reviews*, (2022); e21801. Copyright 2022 Wiley.³⁴

In HDX experiments, differences in the conformations, and potentially the dynamics, of biomolecules are monitored by sampling multiple HDX-labeling times. For in-ESI HDX, differences in the extent of labeling can result from either changing the labeling time, while keeping droplet conditions that affect labeling rates consistent, or altering the rate of exchange, while keeping the labeling time consistent. Prior work has shown that labeling times can be changed by altering the initial size of ESI droplets^{19, 35} or by modulating the rate of droplet evaporation by changing ESI source conditions. ^{16, 17, 20-22, 36} Yet, due to the complex nature of ESI and in-ESI HDX, changing the source conditions often has multifaceted effects on the extent of HDX. ²¹ For example, increasing the ion-tube transfer temperature increases both the rate of ESI-droplet evaporation, decreasing the time for exchange to occur, while also increasing the chemical rate of exchange due to the Arrhenius equation. ^{9, 37}

We propose that the extent of HDX can also be altered by intentionally changing the chemical rate of exchange. This approach is typically utilized in solution-phase exchange only as a mechanism to quench the reaction and cease further exchange of backbone amides. Intrinsic rates of exchange in solution are dependent on pH because exchange for almost all functional groups is catalyzed by both acid and base, ^{32, 38} with the exchange rate minimized at a unique pH for different functional groups. ^{33, 39} In the case of hydroxyls, solution-phase experiments have yielded a minimum rate of HDX around pH 6.5 with the rate of exchange increasing as pH both increases and decreases. In comparison, amides, which form the backbone of peptides and

proteins, experience a minimum rate near pH 2.5, and amines, a common side group on peptides and proteins, do not undergo significant acid catalysis³² and thus experience a consistent, minimal rate of exchange below pH 4.

During ESI, the pH changes; thus, the initial spray-solvent pH and the change in pH during ESI need to be considered for in-ESI HDX experiments. The voltage (kV) applied during ESI is necessary to generate the Taylor cone and ESI droplets; however, this voltage causes oxidation of water within the spray needle, $e.g. 2H_2O \rightarrow 4H^+ + 4e^- + O_2$, leading to solvent acidification in positive-ion mode (**Figure 1**). In nano-ESI experiments using unbuffered solutions, the pH in the ESI tip changes from pH 7 to pH 3 when voltage is applied for 90 minutes due to this redox reaction. Additionally, as ESI droplets desolvate and the volume of individual droplets decreases, H⁺ ions become more concentrated, causing the pH to decrease.

Herein, we investigate the effects of spray solution pH during in-ESI HDX using both carbohydrate- and peptide-model systems. Specifically, we examine how spray-solution pH and buffering capacity affect in-ESI HDX, as well as how altering the spray-solution pH can be used to examine different carbohydrate isomers and small biomolecules, including peptides.

2. Experimental

a. Materials

Melezitose, isomaltotriose, NaCl, and Substance P were from Sigma Aldrich (St. Louis, MO). Maltotriose was from Cayman Chemical (Ann Arbor, MI). Ammonium acetate, NaOH, and HCl were from VWR (Radnor, PA). Deuterium oxide (99.96% purity) was from Cambridge Isotopes (Tewksbury, MA). All chemicals were used without further purification. Nanopure

water was acquired from a Purelab Flex 3 water purification system (Elga, Veolia Environment S. A., Paris, France).

b. Sample Preparation

Carbohydrates were prepared at 250 μM with 1 mM NaCl in nanopure water. Substance P was prepared at 250 μM in nanopure water. pH was adjusted using NaOH or HCl and measured with a Thermo Scientific Orion 8157BNUMD Ross Ultra triode attached to an A215 meter (Thermo-Fisher Scientific, Waltham, MA). For some samples, the conductivity was adjusted using a 0.4 M NaCl stock solution. Sample conductivity was measured after pH adjustment using an Orion 013005MD conductivity probe on the A215 meter. Samples with ammonium acetate (0.1 mM, 10 mM, and 100 mM) were used to examine buffer effects with the buffer added prior to pH and conductivity adjustments.

c. HDX Experiments

In-ESI HDX experiments used a previously published method. ²¹ Briefly, to collect deuterated spectra, the ESI source was saturated with D_2O vapor by placing a droplet of D_2O (200 μ L) on a brass plate in an Ion Max source coupled to an LTQ Discovery (Thermo Fisher, MA). Sample solutions were immediately sprayed and spectra were averaged between 4.0 min and 4.2 min because the $D_2O_{(g)}$ was found to be consistent at this time. ²¹ The D uptake increased over the first 3 minutes of data collection and became repeatable after 3.5 minutes, which is attributed to having a consistent level of $D_2O_{(g)}$ in the source. The following ESI parameters were used – spray voltage: 3.5 kV, sheath gas: 12 arbitrary units, auxiliary gas: 0 arbitrary units, and capillary temperature: 275 °C. Between runs, the source was opened for 5 minutes to remove

residual solvent vapors.^{20, 21} Undeuterated spectra were collected between each deuterated run with neither the D₂O droplet nor the brass plate in the instrument source.

d. Data Processing

The weighted-average mass (M) was calculated for both deuterated and undeuterated sodium-adducted carbohydrates and protonated Substance P using the experimental mass-to-charge (m/z) and intensity (I) of each peak as well as the charge (z) of the analyte ion.

$$M = \frac{\sum (m/z \times I)}{\sum (I)} * z$$
 Eq. 1

D uptake (D) was calculated by subtracting the weighted-average mass of the undeuterated species from the weighted-average mass of the deuterated species.

$$D = M_{Deuterated} - M_{Undeuterated}$$
 Eq. 2

Data are presented as the average $D \pm$ the standard deviation for a minimum of four trials. Statistical analyses (95% confidence interval) used either a Student's or Welch's t-test after standard deviation was assessed using an F test. Data for each figure was collected on a single day.

3. Results and Discussion

a. Carbohydrate HDX is maximized at low pH

To assess the impact of pH during in-ESI HDX, melezitose was sprayed from solutions with varying pH. Initially, similar peak distributions were observed following labeling, with similar levels of D uptake, that were independent of pH (**Figure S1**). Though this data appeared

to contradict solution-phase HDX trends in which pH affected HDX rate, we hypothesize that the similarity in D uptake is the result of competing effects during ESI and in-ESI HDX. For these initial samples, only the pH was adjusted, resulting in different amounts of HCl or NaOH being added to each sample, and leading to different conductivities at each pH (see Table S1). Spraysolvent conductivity affects the initial size of ESI droplets, with higher conductivity solutions producing smaller initial-ESI droplets.^{22, 45} Further, smaller droplets have higher surface tension, which decreases the solubility of gas vapors in droplets^{46, 47} and potentially deceases the amount of D₂O_(l) available for exchange. Smaller ESI droplets evaporate more quickly than larger ESI droplets and result in less time for in-ESI HDX prior to analyte desolvation, when labeling of metal-adducted carbohydrates is effectively quenched. Thus, lower levels of D uptake are expected for analytes in smaller ESI droplets versus analytes in larger ESI droplets.²² Both the highly acidic and highly basic solutions had high conductivity. Alternatively, hydroxyls have a minimum rate of exchange around pH 6.5 with faster exchange rates at more acidic and basic pHs in solution. Thus, if the droplet sizes were consistent at all pH values, we would expect the most D uptake at the highest and lowest pH due to the more rapid rates of HDX. Because pH alters both the droplet sizes, due to differences in conductivity, and exchange rates, these effects appear to negate each other, resulting in similar levels of D uptake for samples sprayed from solutions with different pH and conductivity.

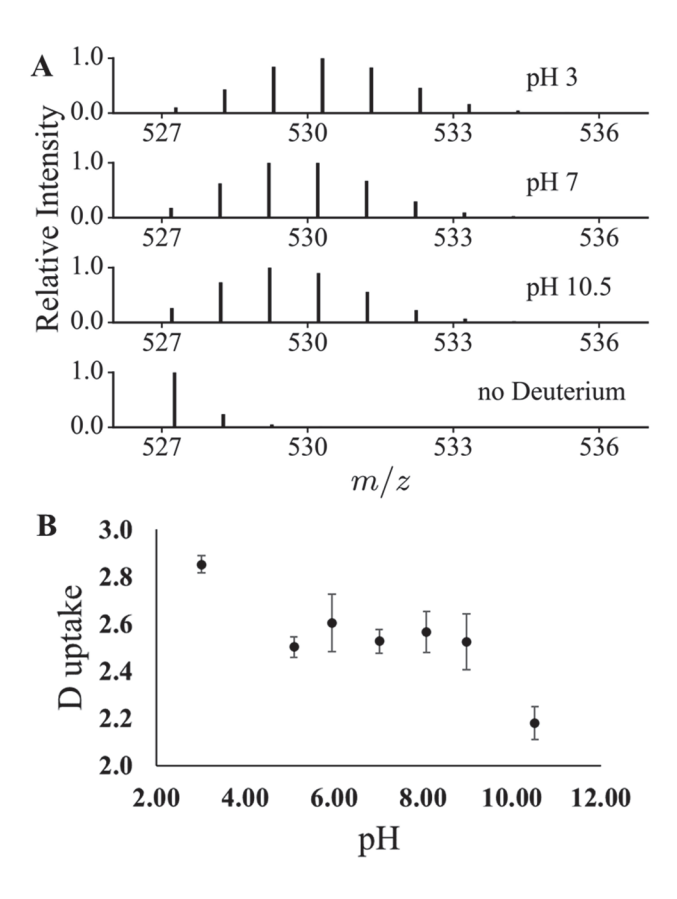


Figure 2. D uptake of sodium-adducted melezitose is dependent on spray solution pH. Representative mass spectra (A) and averaged D uptake (B) for spray solutions with fixed conductivity and different pH. D uptake is highest at low pH, intermediate at a range of mid pH values, and lowest at high pH.

We next examined the effect of solution pH for in-ESI HDX of melezitose when the conductivity of the spray solution was kept consistent between samples (**Table S2**). With fixed conductivities, the representative spectra show differences in the peak distributions following HDX labeling when sprayed from pH 3, 7, and 10.5 (**Figure 2A**). For the pH 10.5 solution, the peak with maximum intensity is at 529.19 *m/z*, while for the pH 3 solution, the peak with

maximum intensity shifts to 530.20 *m/z*. The pH 7 solution has D uptake between these other two solution conditions, with the peaks at both 529.19 *m/z* and 530.20 *m/z* having similar intensities. Overall, **Figure 2B** shows three distinct populations of D uptake, which were statistically different by *t*-test (95% confidence interval), including high D uptake at pH 3, intermediate D uptake between pH 5 to pH 9, and low D uptake at pH 10.5.

D uptake during in-ESI HDX is affected by the spray solution pH. With all solutions having consistent conductivity, we expect the ESI-droplet sizes to be consistent. Thus, the differences in D uptake are attributed to differences in the rate of exchange at each pH. While the rate of exchange during ESI is not expected to be equal to the rate in bulk solution due to the potential for rate acceleration,³⁵ the observed trend in rates of exchange at varying pH were expected to be consistent between in-ESI HDX and bulk-solution HDX. However, unlike in solution, where the rate of exchange for hydroxyls increases at both high and low pH; we observed reduced levels of HDX, which we correlate to slower rates of HDX, at high pH. We hypothesize that the discrepancy between D uptake during in-ESI HDX and solution-phase HDX is due to changes in pH that occur during the ESI process.⁴²

b. Buffer minimizes pH changes during in-ESI HDX.

In ESI, H⁺ is generated when spraying in positive-ion mode (**Figure 1**). Thus, the pH of the spray solvent decreases due to the generation of H⁺ and/or neutralization of OH⁻ within the solution. To further investigate the difference in rates of exchange during in-ESI HDX, we varied the spray solution pH in the presence of ammonium acetate (**Figure 3**). Ammonium acetate was selected as a buffer due to its volatile nature, its frequent use in ESI-MS, and its effective buffering ranges (pK_as 4.75 and 9.25) residing above and below the pH associated with the

minimum rate of HDX for hydroxyls. $^{42,\,48}$ Because positive-ion mode ESI lowers pH by both redox reactions within the spray needle and charge concentration during evaporation of ESI droplets, melezitose solutions were prepared near the high end of the buffer ranges for both acetate and ammonium (pH 6.00 ± 0.01 and pH 10.00 ± 0.01). Furthermore, we altered the ammonium acetate concentration to alter the buffer capacity of the spray solution. We anticipated that the spray solution would start near pH 6 or 10 and experience some level of buffering around pH 4.75 or 9.25 prior to ESI droplet desolvation. Increased buffer capacity is expected to maintain the droplet pH around the pKa of either acetate or ammonium during ESI, 49 , which in turn is expected to enable more confident prediction of the pH surrounding the analyte during in-ESI HDX. This allows for characterization of how ESI affects labeling during in-ESI HDX.

For the samples prepared at pH 6, with no ammonium acetate, 0.1 mM ammonium acetate, and 10 mM ammonium acetate, the measured D uptake was (1.9 ± 0.1) D, (1.6 ± 0.1) D, and (1.11 ± 0.09) D, respectively (**Figure 3A**). Representative mass spectra for each buffer concentration can be seen in **Figure S2**. We expect that as the buffer concentration and buffer capacity increase, the decrease in pH during ESI is reduced (**Figure 3C**). At pH 6.5 the rate of exchange is minimized for hydroxyls in solution. We expect the rate of exchange to increase, resulting in more D uptake, as the pH of the solution decreases below the initial solution pH of 6 due to the ESI process. With increasing buffer concentration, we observe a decrease in D uptake. Thus, even with application of voltage associated with ESI, the increasing buffer concentration and buffer capacity maintain a spray solution pH nearer to that of the starting pH and pH 6.5 where the rate of exchange is minimized, resulting in less D uptake.

For samples prepared at pH 10, with no ammonium acetate, 0.1 mM ammonium acetate, and 10 mM ammonium acetate, the D uptake was (1.93 ± 0.06) D, (1.8 ± 0.2) D, and (2.2 ± 0.2) D, respectively. Representative mass spectra for each buffer concentration can be seen in **Figure S3**. The D uptake for the samples without buffer and with 0.1 mM ammonium acetate were within experimental uncertainty. However, 10 mM ammonium acetate resulted in a significant increase in D uptake compared to the D uptake for samples prepared without buffer and in 0.1 mM ammonium acetate. To further validate this trend, D uptake was measured for melezitose prepared in either a non-buffered solution or 100 mM ammonium acetate. A significant increase in D uptake was observed for melezitose in the buffered solution (**Figure S4**).

We expect that as the buffer concentration and buffer capacity are increased, the decrease in pH during ESI is reduced (**Figure 3C**). However, solutions with high buffer capacity are expected to maintain a pH near 10, while solutions with lower buffer capacity are expected to have a decrease in pH, moving toward pH 6.5 where the rate of HDX for hydroxyls is minimized. When melezitose is prepared in solutions with higher buffer capacity, maintaining a pH near 10, higher D uptake is observed, as expected for the more rapid exchange rate at this pH. In comparison, when melezitose is prepared in solutions with lower buffer capacity, the spray solution pH decreases toward pH 6.5, where the rate of exchange for hydroxyls is minimized and the observed D uptake is reduced.

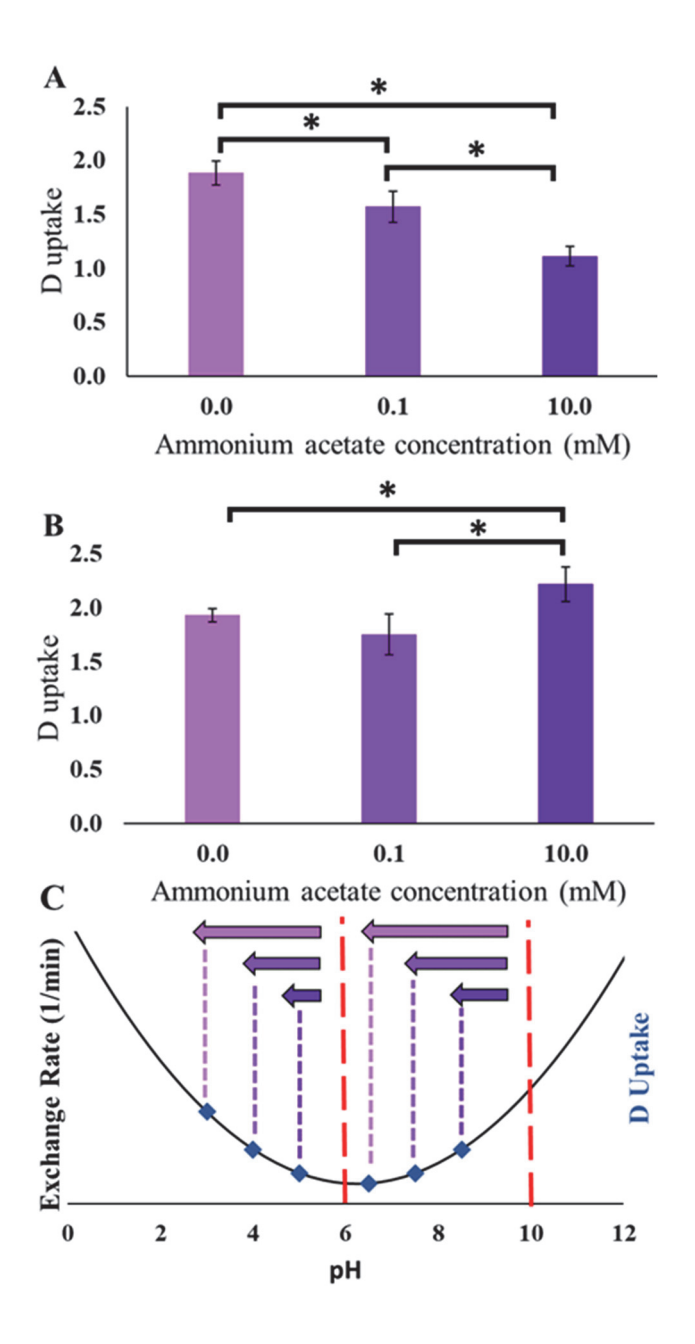


Figure 3. D uptake for sodium-adducted melezitose prepared in spray solutions with varying concentrations of ammonium acetate at either pH 6.00 (A) or 10.00 (B). Conductivity was consistent for solutions at each pH and for all three ammonium acetate concentrations. Stars indicate statistical significance at the 95% confidence interval. (C) Representation of the effects of increasing buffer capacity when spraying solutions with initial pH of either 6 or 10 (red lines). The black curve represents the solution-phase HDX trend for hydroxyls, which have a minimum

rate of exchange at pH 6.5.³² Darker arrow colors represent greater buffer capacity, minimizing the pH change during ESI. When melezitose is sprayed from solutions at pH 6, increasing buffer capacity maintains the solution pH near pH 6.5 where the rate of exchange for hydroxyls is minimized. When melezitose is sprayed from solutions at pH 10, decreasing buffer capacity causes the solution pH to shift toward pH 6.5 where the rate of exchange for hydroxyls is minimized.

The increase in D uptake at pH 10 and the decrease in D uptake at pH 6 as buffer capacity increases supports the hypothesis that in-ESI HDX shows similarities to solution-HDX trends, with exchange catalyzed by both acid and base. Thus, we hypothesize that in negative-ion mode, the increase in pH associated with reduction of water in the spray needle would result in the opposite trends. However, when we prepared solutions with matched conductivities at different pH, we did not observe sufficient analyte signal to test this hypothesis.

c. Trisaccharide isomers can be distinguished with varying spray-solution pH

After observing differences in D uptake based on the pH of the spray solution, we tested whether varying the spray solution pH could be used to distinguish trisaccharide isomers. Previous work from our lab demonstrated that trisaccharide isomers could be distinguished by changing the time for HDX labeling (via controlling the initial size of ESI droplets and, thus, droplet lifetimes).²² Here, rather than controlling the time for exchange, we alter the exchange rate and apply this method to compare the structures and conformations of trisaccharide isomers.

We compared D uptake at low, mid, and high pH for isomaltotriose, maltotriose, and melezitose using in-ESI HDX (**Figure 4**). Maltotriose and isomaltotriose are reducing sugars composed of glucose units connected by α 1-4 and α 1-6 linkages, respectively, while melezitose

is a non-reducing sugar composed of two glucose units connected to an internal fructose. Maltotriose and isomaltotriose are regioisomeric while melezitose differs by both monosaccharide composition and linkage. Similar to the data presented in **Figure 2**, D uptake was highest for all three trisaccharides at low pH, while lower D uptake was observed at both mid and high pH. However, in comparison to **Figure 2**, the D uptake for each trisaccharide was similar when comparing the data collected at pH 6 and 10.5. We attribute this difference in D uptake trends to differences in the conductivity of the analyzed samples. For **Figure 4**, the spray solution had a higher conductivity (**Table S3**) than that used to collect the data presented in **Figure 2**, resulting in smaller initial ESI droplets and less time for labeling.²²

At pH 3, the D uptake of melezitose (3.0 D \pm 0.3 D), isomaltotriose (2.7 D \pm 0.3 D), and maltotriose (3.0 D \pm 0.2 D) were within experimental uncertainties. At pH 6, the D uptake for melezitose (1.6 D \pm 0.2 D) was different from that of isomaltotriose (1.18 D \pm 0.02 D) and maltotriose (1.2 D \pm 0.1 D), but the D uptake for isomaltotriose and maltotriose were within the measurement uncertainty. At pH 10.5, the D uptake for melezitose (1.4 D \pm 0.1 D) was different from that of isomaltotriose (1.09 D \pm 0.03 D), but the D uptake for maltotriose (1.3 D \pm 0.2 D) was within the measurement error for both of the other trisaccharides. Due to the similarities in solution conductivity for all three trisaccharides at all three pHs, the capability of in-ESI HDX to distinguish trisaccharide isomers at varying pH is attributed to differences in exchange rates at each pH, rather than droplet size or gas solubility.^{46,47} The data shown in **Figure 4** suggests that a neutral pH is best for isomer differentiation.

These results indicate that (1) varying the pH of the spray solution during in-ESI HDX allows for unique comparisons of isomeric carbohydrates and (2) utilizing pH to alter the exchange rate of HDX enabled isomers with extensive differences in structure – including

varying monosaccharide units, linkages, and reducing capacity – to be distinguished, though regioisomers were not differentiated here. These results demonstrate that structural differences can be detected through in-ESI HDX by manipulating either the time for HDX by altering the size of the initial ESI droplets,²² or by altering the rate of exchange within the droplets by changing the spray solution pH.

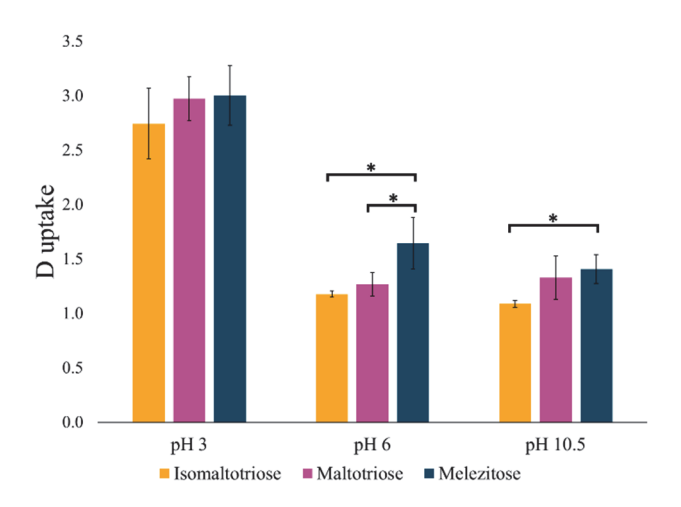


Figure 4. D uptake of sodium-adducted trisaccharide isomers at varying pH. Samples were prepared at each pH in water (without ammonium acetate) and the conductivity for all three trisaccharides at each pH were similar. Stars indicate statistical significance at the 95% confidence interval.

d. Carbohydrates and peptides display different trends in HDX as a result of changing the spray solution pH

Though carbohydrates have been the focus to this point, other biomolecules can be labeled by in-ionization HDX, including metabolites, ^{8, 27, 28} peptides, ³⁵ and proteins. ⁵¹ These molecules contain multiple functional groups with labile H and each functional group has a

distinct trend for exchange rate in relation to pH. Thus, we expect to see different trends in D uptake as the spray solution pH is changed for analytes with varying functional groups. Herein, we compared the D uptake following in-ESI HDX for melezitose and Substance P – an undecapeptide with rapidly exchanging amines and slower exchanging amides. The HDX trend for Substance P is opposite that observed for melezitose, with Substance P showing an increase in D uptake as pH increases while melezitose experiences a decrease in D uptake as pH increases (Figure 5). Representative mass spectra for melezitose and Substance P are presented in Figure S5.

We hypothesize that these different D uptake trends are due to differences in the exchange rate of the different function groups. Carbohydrates are primarily composed of hydroxyls, which exhibit a minimum exchange rate around pH 6.5 with an increase in exchange rate as the solution becomes either more acidic or basic. Peptides contain more diverse functional groups, including amides and amines. Amides have a minimum exchange rate around pH 2.5. Yet, because amides experience slower rates of exchange, on the timescale of milliseconds to seconds in unstructured environments, 32, 38 we expect minimal labeling for amides during ESI.52 Amines exchange on a timescale similar to hydroxyls, between microseconds and milliseconds, but amines have a consistent, minimum exchange rate at or below pH 4.32 For Substance P, the D uptake trend is similar to that expected based on the bulk-solution exchange rates of amines, with the lowest D uptake at pH 3 and increasing D uptake for pH 8 and 10.5. As the pH decreases, the D uptake of Substance P decreases, indicating that exchange occurs at a slower rate. We expect that the pH in ESI droplets decreases because we are once again spraying in positive-ion mode and the spray solution will undergo oxidation due to the applied potential. However, even if the pH decreases from the initial spray solution pH of 3, 8, or 10.5, the exchange rate is still

expected to increase as the pH increases, which is shown in **Figure 5**. For melezitose, which contains multiple hydroxyl functional groups, the ESI process affects the pH and thus the rate of exchange depending upon the starting spray solution pH (**Figure 3C**). The effect of pH on in-ESI HDX rates for different functional groups could provide valuable insight into the identity of the functional groups present within analytes and add additional utility as an orthogonal component of metabolomics workflows.

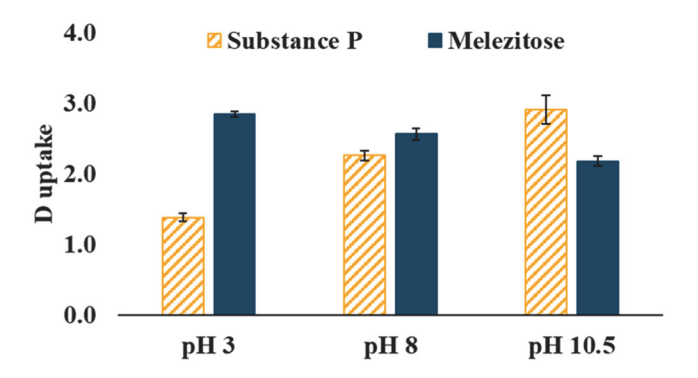


Figure 5. D uptake trends for protonated Substance P and sodium-adducted melezitose at various pH. The conductivity was consistent for both analytes at all pH values. Analytes were sprayed without buffer in the spray solution.

4. Conclusions

In this work, we manipulated the rate of HDX during in-ESI HDX by altering the solution pH and monitored the D uptake for carbohydrates and a model peptide. For carbohydrates, we showed that spray solution pH can have a significant effect on D uptake. The trend in D uptake versus pH was different from that of bulk solution HDX. This is due to the ESI process, in which the applied voltage causes oxidation of water and the evaporation of ESI droplets causes concentration of H⁺, both of which decrease the solution pH. Additionally, it was found that

spray solutions with pH near the minimum HDX rate for hydroxyls, enabled the most distinction between trisaccharide isomers. Alternatively, at low pH, where the HDX rates for hydroxyls are the most rapid, isomers could not be distinguished within measurement uncertainty. Finally, it was found that a model peptide – which primarily experienced exchange at amines during in-ESI HDX – showed a different trend in D uptake at each spray solution pH in comparison to the carbohydrates with hydroxyl functional groups. These results illustrate that the pH of the spray solution should be considered for in-ESI HDX experiments, and that altering the pH during in-ESI HDX may be used to distinguish between different labile functional groups within analytes, including metabolites. Overall, these findings add to the understanding of the complex environment in which in-ESI HDX occurs and point towards increased utility of in-ESI HDX for distinguishing analytes composed of varying functional groups.

5. Acknowledgments

J.B.H. was supported by the National Science Foundation (CHE-1945078) and O.T.L. was supported by the Welch Foundation (AA-1899). We thank the Baylor University Mass Spectrometry Center. We thank our colleagues in the Gallagher and Kane Labs, specifically Ana Quintero and Jessica Kostyo, for useful discussions and feedback.

Supporting Information. Representative mass spectra, plots showing the average D uptake as a function of pH and buffer concentration, and tables of solvent conditions (pH and conductivity) and D uptake values

References

- (1) Varki, A.; Kornfeld, S. Historical Background and Overview. In *Essentials of Glycobiology*, rd, Varki, A., Cummings, R. D., Esko, J. D., Stanley, P., Hart, G. W., Aebi, M., Darvill, A. G., Kinoshita, T., Packer, N. H., et al. Eds.; 2015; pp 1-18.
- (2) Helenius, A. How N-linked oligosaccharides affect glycoprotein folding in the endoplasmic reticulum. *Mol. Biol. Cell* **1994**, *5* (3), 253-265. DOI: 10.1091/mbc.5.3.253.
- (3) Lis, H.; Sharon, N. Protein glycosylation. Structural and functional aspects. *Eur. J. Biochem.* **1993**, *218* (1), 1-27. DOI: 10.1111/j.1432-1033.1993.tb18347.x.
- (4) Moremen, K. W.; Tiemeyer, M.; Nairn, A. V. Vertebrate protein glycosylation: diversity, synthesis and function. *Nat. Rev. Mol. Cell Biol.* **2012**, *13* (7), 448-462. DOI: 10.1038/nrm3383.
- (5) Taniguchi, N.; Kizuka, Y. Chapter Two Glycans and Cancer: Role of N-Glycans in Cancer Biomarker, Progression and Metastasis, and Therapeutics. In *Advances in Cancer Research*, Drake, R. R., Ball, L. E. Eds.; Vol. 126; Academic Press, 2015; pp 11-51.
- (6) Maverakis, E.; Kim, K.; Shimoda, M.; Gershwin, M. E.; Patel, F.; Wilken, R.; Raychaudhuri, S.; Ruhaak, L. R.; Lebrilla, C. B. Glycans in the immune system and The Altered Glycan Theory of Autoimmunity: A critical review. *J. Autoimmu.* **2015**, *57*, 1-13. DOI: 10.1016/j.jaut.2014.12.002.
- (7) Dettmer, K.; Aronov, P. A.; Hammock, B. D. Mass spectrometry-based metabolomics. *Mass Spectrom. Rev.* **2007**, *26* (1), 51-78. DOI: 10.1002/mas.20108.
- (8) Majuta, S. N.; Li, C.; Jayasundara, K.; Kiani Karanji, A.; Attanayake, K.; Ranganathan, N.; Li, P.; Valentine, S. J. Rapid Solution-Phase Hydrogen/Deuterium Exchange for Metabolite Compound Identification. *J. Am. Soc. Mass Spectrom.* **2019**, *30* (6), 1102-1114. DOI: 10.1007/s13361-019-02163-0.
- (9) Oganesyan, I.; Lento, C.; Wilson, D. J. Contemporary hydrogen deuterium exchange mass spectrometry. *Methods* **2018**, *144*, 27-42. DOI: 10.1016/j.ymeth.2018.04.023.
- (10) Linderstrom-Lang, K. Deuterium exchange and protein structure. *Symp. Protein Struct.* **1958**, *9*, 23-34.
- (11) Pan, J.; Heath, B. L.; Jockusch, R. A.; Konermann, L. Structural Interrogation of Electrosprayed Peptide Ions by Gas-Phase H/D Exchange and Electron Capture Dissociation Mass Spectrometry. *Anal. Chem.* **2012**, *84* (1), 373-378. DOI: 10.1021/ac202730d.
- (12) Hemling, M. E.; Conboy, J. J.; Bean, M. F.; Mentzer, M.; Carr, S. A. Gas-Phase Hydrogen-Deuterium Exchange in Electrospray-Ionization Mass-Spectrometry as a Practical Tool for Structure Elucidation. *J. Am. Soc. Mass Spectrom.* **1994**, *5* (5), 434-442. DOI: 10.1016/1044-0305(94)85059-3.
- (13) Kelly, K.; Bell, S.; Maleki, H.; Valentine, S. Synthetic Small Molecule Characterization and Isomer Discrimination Using Gas-Phase Hydrogen–Deuterium Exchange IMS-MS. *Anal. Chem.* **2019**, *91* (9), 6259-6265. DOI: 10.1021/acs.analchem.9b00979.
- (14) Price, N. P. Oligosaccharide structures studied by hydrogen-deuterium exchange and MALDI-TOF mass spectrometry. *Anal. Chem.* **2006**, *78* (15), 5302-5308. DOI: 10.1021/ac052168e.
- (15) Guttman, M.; Scian, M.; Lee, K. K. Tracking hydrogen/deuterium exchange at glycan sites in glycoproteins by mass spectrometry. *Anal. Chem.* **2011**, *83* (19), 7492-7499. DOI: 10.1021/ac201729v.

- (16) Kostyukevich, Y.; Kononikhin, A.; Popov, I.; Nikolaev, E. Conformations of cationized linear oligosaccharides revealed by FTMS combined with in-ESI H/D exchange. *J. Mass Spectrom.* **2015**, *50* (10), 1150-1156. DOI: 10.1002/jms.3633.
- (17) Kostyukevich, Y.; Kononikhin, A.; Popov, I.; Nikolaev, E. In-ESI source hydrogen/deuterium exchange of carbohydrate ions. *Anal. Chem.* **2014**, *86* (5), 2595-2600. DOI: 10.1021/ac4038202.
- (18) Uppal, S. S.; Beasley, S. E.; Scian, M.; Guttman, M. Gas-Phase Hydrogen/Deuterium Exchange for Distinguishing Isomeric Carbohydrate Ions. *Anal. Chem.* **2017**, *89* (8), 4737-4742. DOI: 10.1021/acs.analchem.7b00683.
- (19) Kim, H. J.; Gallagher, E. S. Achieving multiple hydrogen/deuterium exchange timepoints of carbohydrate hydroxyls using theta-electrospray emitters. *Analyst* **2020**, *145* (8), 3056-3063. DOI: 10.1039/d0an00135j.
- (20) Kim, H. J.; Liyanage, O. T.; Mulenos, M. R.; Gallagher, E. S. Mass Spectral Detection of Forward- and Reverse-Hydrogen/Deuterium Exchange Resulting from Residual Solvent Vapors in Electrospray Sources. *J. Am. Soc. Mass Spectrom.* **2018**, *29* (10), 2030-2040. DOI: 10.1007/s13361-018-2019-6.
- (21) Liyanage, O. T.; Brantley, M. R.; Calixte, E. I.; Solouki, T.; Shuford, K. L.; Gallagher, E. S. Characterization of Electrospray Ionization (ESI) Parameters on In-ESI Hydrogen/Deuterium Exchange of Carbohydrate-Metal Ion Adducts. *J. Am. Soc. Mass Spectrom.* **2019**, *30* (2), 235-247. DOI: 10.1007/s13361-018-2080-1.
- (22) Liyanage, O. T.; Quintero, A. V.; Hatvany, J. B.; Gallagher, E. S. Distinguishing Carbohydrate Isomers with Rapid Hydrogen/Deuterium Exchange-Mass Spectrometry. *J. Am. Soc. Mass Spectrom.* **2021**, *32* (1), 152-156. DOI: 10.1021/jasms.0c00314.
- (23) Liyanage, O. T.; Seneviratne, C. A.; Gallagher, E. S. Applying an Internal Standard to Improve the Repeatability of In-electrospray H/D Exchange of Carbohydrate-Metal Adducts. *J. Am. Soc. Mass Spectrom.* **2019**, *30* (8), 1368-1372. DOI: 10.1007/s13361-019-02153-2.
- (24) Hatvany, J. B.; Gallagher, E. S. Hydrogen/deuterium exchange for the analysis of carbohydrates. *Carbohydrate Research* **2023**, *530*, 108859. DOI: 10.1016/j.carres.2023.108859.
- (25) Mookherjee, A.; Uppal, S. S.; Guttman, M. Dissection of Fragmentation Pathways in Protonated N-Acetylhexosamines. *Anal. Chem.* **2018**, *90* (20), 11883-11891. DOI: 10.1021/acs.analchem.8b01963.
- (26) Mookherjee, A.; Uppal, S. S.; Murphree, T. A.; Guttman, M. Linkage Memory in Underivatized Protonated Carbohydrates. *J. Am. Soc. Mass Spectrom.* **2020**, *32* (2), 581-589. DOI: 10.1021/jasms.0c00440.
- (27) DeBastiani, A.; Majuta, S. N.; Sharif, D.; Attanayake, K.; Li, C.; Li, P.; Valentine, S. J. Characterizing Multidevice Capillary Vibrating Sharp-Edge Spray Ionization for In-Droplet Hydrogen/Deuterium Exchange to Enhance Compound Identification. *ACS Omega* **2021**, *6* (28), 18370-18382. DOI: 10.1021/acsomega.1c02362.
- (28) Song, X.; Li, J.; Mofidfar, M.; Zare, R. N. Distinguishing between Isobaric Ions Using Microdroplet Hydrogen–Deuterium Exchange Mass Spectrometry. *Metabolites* **2021**, *11* (11). DOI: 10.3390/metabo11110728.
- (29) Calixte, E. I.; Liyanage, O. T.; Gass, D. T.; Gallagher, E. S. Formation of Carbohydrate–Metal Adducts from Solvent Mixtures during Electrospray: A Molecular Dynamics and ESI-

- MS Study. *Journal of the American Society for Mass Spectrometry* **2021**, *32* (12), 2738-2745. DOI: 10.1021/jasms.1c00179.
- (30) Oganesyan, I.; Hajduk, J.; Harrison, J. A.; Marchand, A.; Czar, M. F.; Zenobi, R. Exploring Gas-Phase MS Methodologies for Structural Elucidation of Branched N-Glycan Isomers. *Anal. Chem.* **2022**, *94* (29), 10531-10539. DOI: 10.1021/acs.analchem.2c02019.
- (31) Tittebrandt, S.; Edelson-Averbukh, M.; Spengler, B.; Lehmann, W. D. ESI Hydrogen/Deuterium Exchange Can Count Chemical Forms of Heteroatom-Bound Hydrogen. *Angewandte Chemie International Edition* **2013**, *52* (34), 8973-8975. DOI: 10.1002/anie.201304249.
- (32) Hamuro, Y. Tutorial: Chemistry of Hydrogen/Deuterium Exchange Mass Spectrometry. *J. Am. Soc. Mass Spectrom.* **2021**, *32* (1), 133-151. DOI: 10.1021/jasms.0c00260.
- (33) Englander, S. W.; Kallenbach, N. R. Hydrogen exchange and structural dynamics of proteins and nucleic acids. *Quart. Rev. Biophys.* **1983**, *16* (4), 521-655. DOI: 10.1017/S0033583500005217.
- (34) Gass, D. T.; Quintero, A. V.; Hatvany, J. B.; Gallagher, E. S. Metal adduction in mass spectrometric analyses of carbohydrates and glycoconjugates. *Mass Spectrom. Rev.* **2022**, e21801. DOI: 10.1002/mas.21801.
- (35) Jansson, E. T.; Lai, Y. H.; Santiago, J. G.; Zare, R. N. Rapid Hydrogen-Deuterium Exchange in Liquid Droplets. *J. Am. Chem. Soc.* **2017**, *139* (20), 6851-6854. DOI: 10.1021/jacs.7b03541.
- (36) Kostyukevich, Y.; Kononikhin, A.; Popov, I.; Nikolaev, E. Simple atmospheric hydrogen/deuterium exchange method for enumeration of labile hydrogens by electrospray ionization mass spectrometry. *Anal. Chem.* **2013**, *85* (11), 5330-5334. DOI: 10.1021/ac4006606.
- (37) Englander, S. W. Hydrogen exchange and mass spectrometry: A historical perspective. *J Am Soc Mass Spectrom* **2006**, *17* (11), 1481-1489. DOI: 10.1016/j.jasms.2006.06.006.
- (38) Bai, Y.; Milne, J. S.; Mayne, L.; Englander, S. W. Primary structure effects on peptide group hydrogen exchange. *Proteins* **1993**, *17* (1), 75-86. DOI: 10.1002/prot.340170110.
- (39) Liepinsh, E.; Otting, G. Proton exchange rates from amino acid side chains—implications for image contrast. *Magn. Reson. Med.* **1996**, *35* (1), 30-42. DOI: 10.1002/mrm.1910350106.
- (40) Van Berkel, G. J.; Zhou, F.; Aronson, J. T. Changes in bulk solution pH caused by the inherent controlled-current electrolytic process of an electrospray ion source. *Int. J. Mass Spectrom. Ion Proc.* **1997**, *162* (1), 55-67. DOI: 10.1016/S0168-1176(96)04476-X.
- (41) Van Berkel, G. J.; Asano, K. G.; Schnier, P. D. Electrochemical processes in a wire-in-acapillary bulk-loaded, nano-electrospray emitter. *J. Am. Soc. Mass Spectrom.* **2001**, *12* (7), 853-862. DOI: 10.1016/S1044-0305(01)00264-1.
- (42) Konermann, L. Addressing a Common Misconception: Ammonium Acetate as Neutral pH "Buffer" for Native Electrospray Mass Spectrometry. *J. Am. Soc. Mass Spectrom.* **2017**, *28* (9), 1827-1835. DOI: 10.1007/s13361-017-1739-3.
- (43) Zhou, S.; Prebyl, B. S.; Cook, K. D. Profiling pH Changes in the Electrospray Plume. *Anal. Chem.* **2002**, *74* (19), 4885-4888. DOI: 10.1021/ac025960d.
- (44) Girod, M.; Dagany, X.; Antoine, R.; Dugourd, P. Relation between charge state distributions of peptide anions and pH changes in the electrospray plume. A mass spectrometry and optical spectroscopy investigation. *International Journal of Mass Spectrometry* **2011**, *308* (1), 41-48. DOI: 10.1016/j.ijms.2011.07.020.

- (45) de Juan, L.; de la Mora, J. F. Charge and Size Distributions of Electrospray Drops. *J. Colloid Interf. Sci.* **1997**, *186* (2), 280-293. DOI: 10.1006/jcis.1996.4654.
- (46) Tolman, R. C. The Effect of Droplet Size on Surface Tension. *The Journal of Chemical Physics* **2004**, *17* (3), 333-337. DOI: 10.1063/1.1747247.
- (47) Uhlig, H. H. The Solubilities of Gases and Surface Tension. *The Journal of Physical Chemistry* **1937**, *41* (9), 1215-1226. DOI: 10.1021/j150387a007.
- (48) Kebarle, P.; Verkerk, U. H. Electrospray: from ions in solution to ions in the gas phase, what we know now. *Mass Spectrom. Rev.* **2009**, *28* (6), 898-917. DOI: 10.1002/mas.20247.
- (49) Gadzuk-Shea, M. M.; Hubbard, E. E.; Gozzo, T. A.; Bush, M. F. Sample pH Can Drift during Native Mass Spectrometry Experiments: Results from Ratiometric Fluorescence Imaging. *Journal of the American Society for Mass Spectrometry* **2023**, *34* (8), 1675-1684. DOI: 10.1021/jasms.3c00147.
- (50) Konermann, L.; Liu, Z.; Haidar, Y.; Willans, M. J.; Bainbridge, N. A. On the Chemistry of Aqueous Ammonium Acetate Droplets during Native Electrospray Ionization Mass Spectrometry. *Anal. Chem.* **2023**, *95* (37), 13957-13966. DOI: 10.1021/acs.analchem.3c02546.
- (51) Sanguantrakun, N.; Chanthamontri, C.; Gross, M. L. Top-Down Analysis of In-Source HDX of Native Protein Ions. *J. Am. Soc. Mass Spectrom.* **2020**, *31* (5), 1151-1154. DOI: 10.1021/jasms.9b00149.
- (52) Sharif, D.; Rahman, M.; Mahmud, S.; Sultana, M. N.; Attanayake, K.; DeBastiani, A.; Foroushani, S. H.; Li, P.; Valentine, S. J. In-droplet hydrogen–deuterium exchange to examine protein/peptide solution conformer heterogeneity. *Rapid Commun. Mass Spectrom.* **2023**, *37* (16), e9593. DOI: 10.1002/rcm.9593.

TOC Figure/Abstract Graphic

